Improving Stability of Tumor Suppressor Protein, p53

Senior Honors Thesis

Presented in Partial Fulfillment of the Requirements for graduation with distinction in Biochemistry in the undergraduate colleges of The Ohio State University

by

Matthew Michael Heberling

The Ohio State University
June 2007

Committee:
Prof. Thomas J. Magliery, Advisor
Prof. Mark P. Foster
Prof. Michael G. Poirier

ACKNOWLEDGEMENTS

Ruth Nussinov, collaborator (NCI- Frederick, Frederick, Maryland)

Dr. Thomas J. Magliery, Research Adviser, The Ohio State University Department of Chemistry and Biochemistry

Dr. Mark P. Foster, oral exam committee, The Ohio State University Department of Biochemistry

Dr. Michael G. Poirier, oral exam committee, The Ohio State University Department of Physics

Funding:

College of Arts and Sciences Research Scholarship

Summer Undergraduate Research Program (SURP), Ohio State University Department of Biochemistry

Dean's Undergraduate Research Grant, College of Biological Sciences

Louis G. Bernstein Memorial Scholarship

ABSTRACT

Tumor suppressor protein p53 is a critical transcription factor involved in an intricate signaling network responsible for cell fate. In over half of all human cancers, p53 is found inactivated from missense mutations and is only marginally stable at physiological conditions. Therefore, immense research has become focused on stabilizing p53. This study intends to test two p53 mutants for relative stability based on prior computational predictions that involved a previously engineered 'super-stable' mutant and a simulated loop deletion mutant, which is predicted to be more stable. Based on protein purification observations for both mutants, significant differences in structural features seem apparent, even before detailed biophysical characterization. The significance of this study is twofold. First, this work may initiate similar studies to ultimately impact the reliability on computational predictions for molecular stability, possibly leading to a widespread use for high throughput analysis of biomolecules. Finally, we may be able to develop insight for additional stabilizing forces of p53 that may enhance therapeutic drug design for many cancer types.

CHAPTER 1. OVERVIEW

1.1 Introduction

Mutational analysis has become a key mechanism for understanding the structure-function interplay within proteins. In general, proteins with a relatively simple structure and of manageable size are often the desired features to perform mutation studies that may serve as a model for other protein families. With such parameters, the core domain of protein, p53, has received significant attention. P53 holds a multi-faceted functionality related to cell-cycle control and ultimately, cancer. P53 has been referred to as a guardian of the genome, having evolved as a transcription factor responsible for promoting expression of the regulatory genes directly involved in cell-cycle arrest, apoptosis (programmed cell death), and the preclusion of angiogenesis.[4] P53 achieves this role through its position in an intricate network that is elicited upon cell stress from UV light, oncogenes, and DNA damage (**Fig. 1**).[6] Disruption of this hub can destroy the intimate network that supports basic cellular functions.

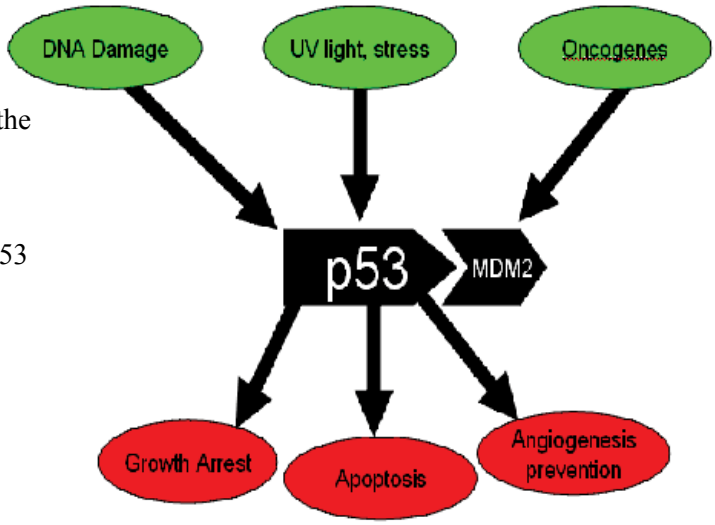

Figure 1. The p53 network. Three independent pathways exist that activate the p53 network in response to cell stress. Mdm2 serves as a negative regulator of p53 by tagging it for proteolysis (protein degradation), thereby controlling physiological concentrations of p53.[2]

1.2 Structural Features of p53. P53 is made up of 393 amino acids within three domains: (1) the N-terminal domain contains transactivation activity for regulatory purposes (e.g.,

interactions with negative regulator, Mdm2 (**Fig. 1**)); (2) the C-terminal domain that entails two sub-domains called the tetramerization domain, which modulates oligomerization, and an auto-regulatory domain involved in non-specific DNA binding through acetylation; and (3) the DNA binding domain, or core domain (p53c), that contains predominantly β-sheet structure and binds specific DNA sites for transcriptional control of the p53 network.[2, 7, 8] Among the three domains, p53c and the tetramerization domains are the key domains that provide structural insight because of their intrinsic order through α-helical and β-sheet features. All other domains are naturally disordered and unfolded.[9]

1.3 Cancerous Mutations of p53. P53 is only marginally stable at physiological conditions (~6 kcal mol^{-1}); exposing key residues to debilitating mutations.[5] Mutations of the p53 gene are observed in almost half of all human cancers.[10]

Of these cancerous mutations, the majority have been mapped to the core domain (**Fig. 2**).[11]

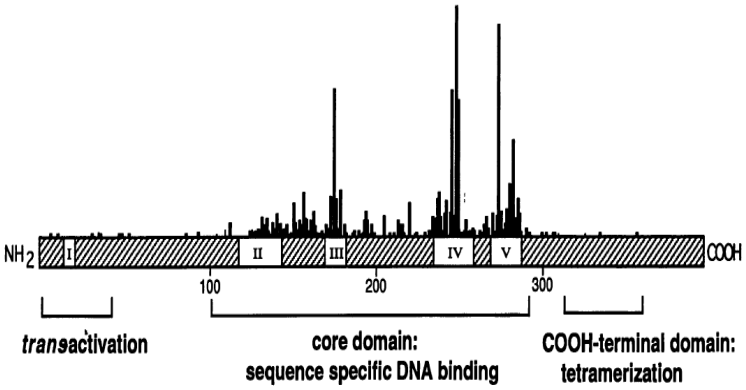

(Cho et al., 1994)

Figure 2. The five highly conserved regions of the p53 gene across species are indicated by roman numerals. The bar graph depicts the predominant frequency of tumor-derived mutations contained within the core domain relative to the other two domains.

The major core domain mutations (residues 175, 243, 245, 248, 249, 273, and 282) can be classified as either thermodynamic or contact mutants (**Fig. 3**).[7] The DNA contact mutants (Arg^{273}, Arg^{248}, and Arg^{280}) have been shown to slightly reduce thermodynamic stability, but

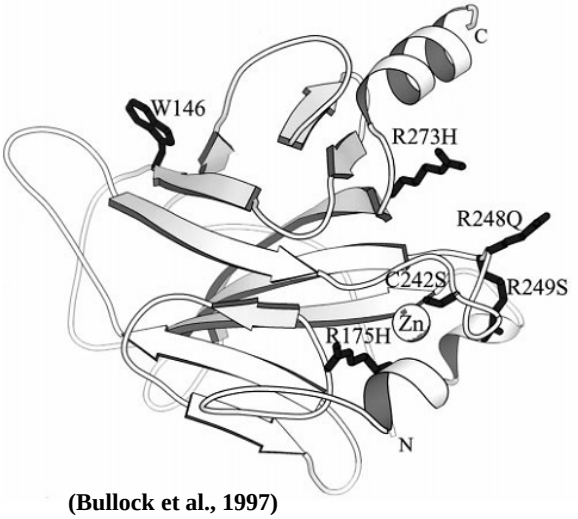

(Bullock et al., 1997)

Figure 3. MOLSCRIPT[1] cartoon of "hot spot" mutations within p53 core domain. Zinc-binding ligand mutants, R175H and C242S, have been shown to be destabilized by approximately ~ 3 kcal mol^{-1}. DNA contact mutation, R248Q, and structural mutation, R249S, are represented in proximity to the zinc finger motif. Trp^{146} is the fluorescing residue used for denaturation experiments .[3, 5]

substantially compromise DNA binding without structural perturbation**.**[12, 13] A hybrid mutation that affects not only DNA contact, but also dimerization between two core domains, is located in the L3 loop, which contains one DNA contact residue, Arg^{248}. [14] When structural mutations arise within this loop (G245S and R249S), a loss of DNA contact via Arg^{248} results in functional and enthalpic costs. Temperature-sensitive mutant, R175H, is the most common cancerous mutation that involves interference with three proximal zinc-binding ligands that result in a loss of key electrostatic interactions.[15]

1.4 Thermostability of p53. The marginal stability of p53 serves as the major reason for its high sensitivity to mutations that result in reduced driving forces for folding to a functional state. Due to the high frequency of cancerous mutations within the core domain (p53c), Niklova et al. have engineered a p53c mutant based on statistical analysis of conserved residues and a prior knowledge of rescue mutations.[16] The mutant was shown to stabilize the core domain by 2.65 kcal mol^{-1}. This "super-stable" mutant has four mutations (M133L/V203A/N239Y/N268D) incorporated throughout the β-sheet scaffold, which has

been coined as the "quad mutant." The quad mutant consists of two second-site suppressor mutations previously shown to rescue DNA contact mutants, G245S and R249S (**Fig. 3**), through global stabilization.[17] A subsequent study mapped these quadruple mutations to the full-length protein (T-p53FL) in order to perform concurrent thermodynamic studies between isolated quad mutant core domains (T-p53C).[3] Each of the six common cancer mutations (**1.3**) were separately incorporated into the core domain and full-length protein for thermodynamic comparison via Differential Scanning Calorimetry (DSC) (**Fig. 4**). Urea-induced denaturation studies using Trp^{146} (**Fig. 3**) as a fluorescence probe was not used since full-length contains three interfering N-terminus Trp residues. Their findings (**Fig. 4**) indicate a substantial influence of the core domain on overall thermostability of the full-length protein through similar apparent melting temperatures (T_m). For instance, when structural hot spot mutation, G245S, is present in full-length p53 (T-p53-G245S) and the isolated core domain ([T-p53C]G245S), each apparent T_m are virtually the same: 47.3 ± 0.3 ºC for full-length and 47.3 ± 0.2 ºC for the isolated core domain. Therefore, studies that use only isolated core

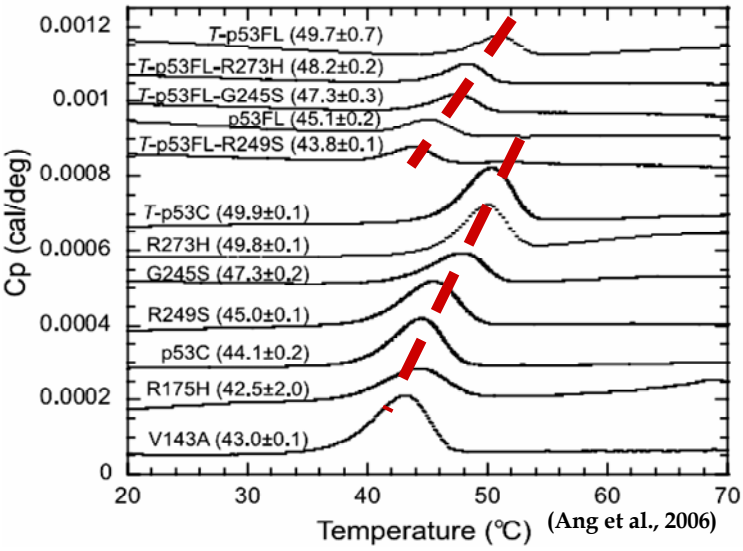

Figure 4. Differential Scanning Calorimetry (DSC) thermal studies. Thermostable full-length p53 (T-p53-FL) and thermostable p53 core domains (T-p53C) were tested for correlated thermostability upon separate mutation with hot spot cancerous mutations.[3]

domains to probe the thermodynamic effects of mutations are adequately justified without a comparison to full-length p53.

1.5 DNA Recognition by p53.

The highly disordered regions of tetrameric p53 (N-terminus) and its size (170 kDa) are the major limitations in obtaining crystallization and NMR studies, respectively, to elucidate exact domain conformations upon DNA binding. However, one study confirmed that the DNA binding domain (p53c) cooperatively binds in a tetrameric complex upon each domain specifically recognizing decameric half-site motifs 5'-Pu·Pu·Pu·C·(A/T)·(A/T)·G·Py· Py·Py·-3'with a 0-13 base pair separation.[18] The DNA recognition site acts a as a glue to form a dimer, which has been confirmed by NMR and mutagenesis/binding studies.[19] Two types of protein-protein interfaces exist within p53 tetramers: (i) dimer interface between core domains; and (ii) tetramerization interface. Mutations of the core domain interactions (i) (e.g., structural hot spot mutations, **1.3**) involve highly conserved residues and are prevalent in many human cancers, whereas residues in the tetramerization interface (translational interface) show high variability. The translational interface is thought to be modulated by the DNA substrate in addition to other protein interactions.[14] Considering the highly conserved dimer interface and its major influence on DNA binding of p53, it is apparent how destabilizing structural mutations within the dimer interface (inter-core domain interactions) have a profound effect on the overall p53 structure, ultimately compromising function with cancerous effects.

1.6 Computational Predictions Suggest Stabilizing Mutants. Molecular dynamic (MD) simulations provide insight to structural fluctuations within molecules as a function of time based on a computer algorithm (e.g. CHARMM).[20] A major advantage to this approach is the

ability to calculate properties of a molecule that are hard to measure empirically. One study administered MD simulations for a comparison between *C. elegans* (worm) and the human core domain.[21] *C. elegans* p53 (p53w), an analog to human p53 (p53h), has been shown to have similar DNA-binding functionality as the human p53.[22] Both core domains have similar structural homology as well (**Fig. 5**).[23] Therefore, this study explored the subtle structural differences between human and worm core domains to elucidate potential enhancements of stability of the human p53 core domain. The simulations (**Fig. 6**) indicate p53w exhibits less structural fluctuations relative to p53h over the same timescale (5 ns). Upon residue-specific simulations, the S7S8 turn in p53h is postulated to contribute substantially to the overall domain instability of p53h. Therefore, shortening the S7S8 (P223A followed by a loop deletion of Glu224, Val225, Gly226, Ser227, and Asp228) loop is predicted to surpass wild-type human stability. Simulations tested the loop mutant against other human core domain mutants, including the quad mutant (**1.4**), and worm. The results (**Fig. 7**) suggest the loop mutant to surpass the quad mutant in stability.

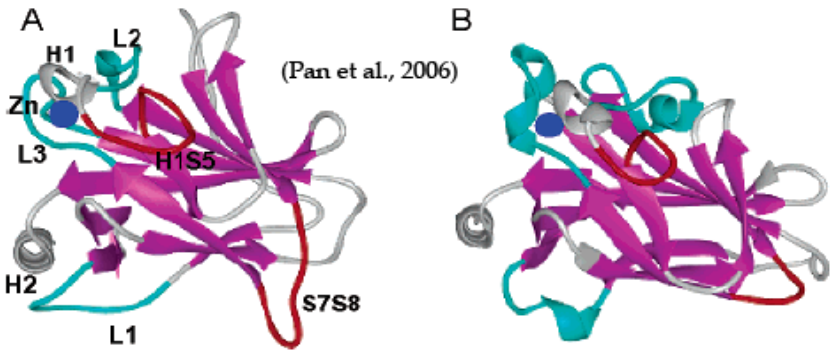

Figure 5. Topological similarities between p53h (**A**) and p53w (**B**) core domains outlined by ribbon structures. Loops L1 and S7S8 are longer in human p53, but overall topology very similar.

Figure 6. MD simulation studies compare structural fluctuations over time for the core domains of **human** and **worm** p53 at 300K (**A**) and 325K (**B**). The plots indicate relative kinetic instability of **p53h** (**black**) at both temperatures compared to **p53w** (**red**).

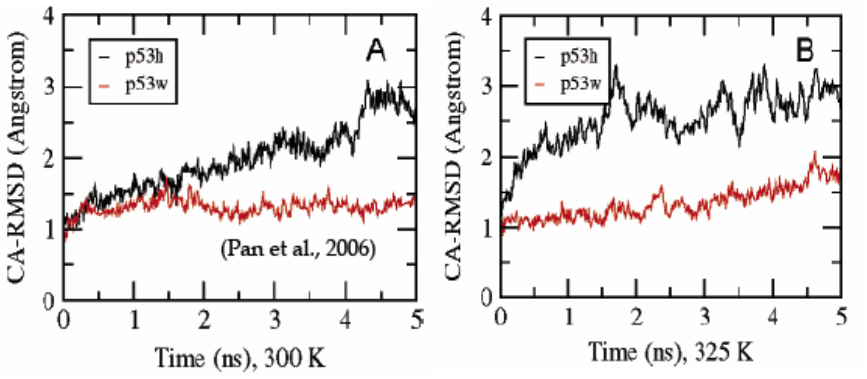

Figure 7. MD simulation studies compare structural fluctuations over time for p53 human core domain mutants and **worm**. Results indicate **Loop S7S8** mutant to surpass **quad** mutant in stability.

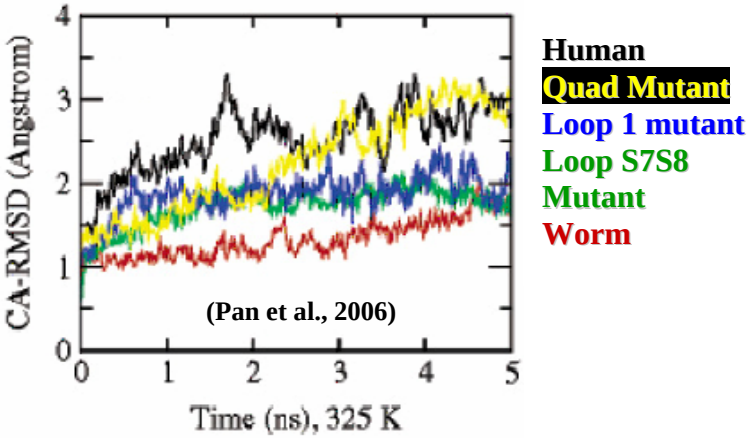

1.7 Objective. Given the prominent role of the human p53 core domain and its effects on full-length p53, both functionally and thermodynamically, the overarching goal of this study is to test both the quad mutant (**1.4**) and loop mutant (**1.5**) for relative thermodynamic stability via urea-induced and thermal denaturation studies; and perform biophysical studies using NMR, Circular Dichroism (CD) Spectroscopy, and Hydrogen/Deuterium (H/D) Exchange for structural characterization. In general, this study is testing for actual relative stabilities to corroborate computational predictions. We hope to obtain biophysical measurements for elucidating the features responsible for the stability variances.

CHAPTER 2. MATERIALS AND METHODS

2.1 p53c Gene Subcloning. The segment of the human p53 core domain gene encoding

residues 94-289 was synthesized using PCR for gene-overlap reassembly of 10 oligonucleotides (Sigma-Genosys) ranging from 50 to 94 nucleotides (**Table 1**) with a 20-nucleotide overlap .[7] Mutations of the loop and quad mutants (**Table 2**) were synthesized in separate oligonucleotides and replaced the respective non-mutated fragment for the gene reassembly reaction. Each primer was prepared to give a 100 μM stock solution in dH_20. The gene reassembly mixture to be used in the PCR gene reassembly reaction consisted of each oligonucleotide to give a total volume of 50 μL (10 μM of each primer). PCR conditions with a PTC-200 Peltier Thermal Cycler for the gene reassembly are: 81.5 μL dH_20, 10 μL 10x Taq Polymerase Buffer (NEB), 2.5 μL dNTP mix (25 μM of each nucleotide, NEB), 5 μL reassembly mixture, 1 μL Taq polymerase (NEB); denaturation- 94 ºC, 2 min, 59 cycles consisting of (i) denaturation 94 ºC; 30 s; (ii) annealing 55 ºC, 45 s; and (iii) extension 72 ºC, 50 s. Final extension was 72 ºC for 2 min. PCR conditions with a PTC-200 Peltier Thermal Cycler for the amplification of gene reassembly are: 41.5 μL dH_20, 5 μL 10x Thermopol Buffer (NEB), 1 μL dNTP mix (25 μM of each nucleotide, NEB), 1 μL forward primer, 1 μL reverse primer, and 1 μL Deep Vent polymerase (NEB); initial denaturation 94 ºC, 2 min, 29 cycles consisting of (i) denaturation 95 ºC, 30 s; (ii) annealing 62.5 ºC, 45 s; and (iii) extension 72 ºC, 60 s. Final extension was 72 ºC for 5 min. The gene reassembly reaction was amplified by PCR by using the oligonucleotides 5'-AAT AAT AAT CAT ATG GCG CAT CAC CAT CAC CAT CAC GGC GGC GAA AAT CTA TAT TTC CAA GCT AGC TCT AGC GTG CCG AGC -3' and 5'-ATT ATT GGA TCC TTA CAG GTT CTC CTC TTC GGT AC-3'. The forward primer contains an N-terminal fusion of 6xHis/TEV cleavage/linker sequence. The p53c gene was digested with *Nde*I and *Bam*HI (NEB) restriction enzymes and subcloned into pET11a containing lacI, ColE1 ori,

p53c human wt

#1	5'-AGCTCTAGCGTGCCGAGCCAGAAAACCTATCAGGGCAGCTATGGCTTTCG-3'
#2	5'-CAGTGCCGGGCTATAGGTACAGGTCACGCTCTTTGCGGTGCCGCTATGCAGAAAG CCCAGACGAAAGCCATAGCTGCCCTG-3'
#3	5'-GTACCTATAGCCCGGCACTGAATAAAATGTTTTGTCAGCTGGCAAAGACCTGTCCGG TGCAGCTGTGGGTGGATAGCACCCCGCCAC-3'
#4	5'-CCACTTCGGTCATGTGCTGGCTCTGTTTATAAATTGCCATTGCACGCACACGGGTGCC CGGTGGCGGGGTGCTATCCAC-3'
#5	5'-GCCAGCACATGACCGAAGTGGTGCGTCGTTGTCCGCATCATGAACGTTGTAGCGATAG-3'
#6	5'-GACGGAAGGTGTTACGATCATCCAGATATTCCACACGCAGATTGCCTTCCACACGAA TCAGATGCTGCGGCGGTGC-3'
#7	5'-GATGATCGTAACACCTTCCGTCATAGCGTGGTTGTGCCGTATGAACCGCCGGAAGTG GGCAGCGATTGTACCACCATTCACTACAACTACATG-3'
#8	5'-GGTCAGGATCGGACGACGATTCATGCCGCCCATACAGCTGCTATTACACATGTAGTT GTAGTGAATGGTGGTAC-3'
#9	5'-CGTCGTCCGATCCTGACCATTATTACCCTGGAAGATAGCAGCGGCAATCTGCTGGG CCGTAATAGCTTCGAGGTGCG-3'
#10	5'-CAGGTTCTCCTCTTCGGTACGACGATCACGGCCCGGACATGCACACACACGCACCT CGAAGCTATTACGG-3'

p53c P223A ΔS7S8 (loop mutant)

#7a	5'-GATGATCGTAACACCTTCCGTCATAGCGTGGTTGTGCCGTATGAACCG**GCA**TGTACC ACCATTCACTACAACTACATG-3'

P53c Quad Mutant

#3q	5'-GTACCTATAGCCCGGCACTGAATAAA**CTG**TTTTGTCAGCTGGCAAAGACCTGTCCGGT GCAGCTGTGGGTGGATAGCACCCCGCCAC-3'
#6q	5'-GACGGAAGGTGTTACGATCATCCAGATATTC**CGC**ACGCAGATTGCCTTCCACACGAAT CAGATGCTGCGGCGGTGC-3'
#8q	5'-GGTCAGGATCGGACGACGATTCATGCCGCCCATACAGCTGCT**GTA**ACACATGTAGTT GTAGTGAATGGTGGTAC-3'
#9q	5'-CGTCGTCCGATCCTGACCATTATTACCCTGGAAGATAGCAGCGGCAATCTGCTGGGC CGT**GAT**AGCTTCGAGGTGCG-3'
#10q	5'-CAGGTTCTCCTCTTCGGTACGACGATCACGGCCCGGACATGCACACACACGCACC TCGAAGCT**ATC**ACGG-3'

Table 1. Overlap gene reassembly primers. Oligonucleotide primers for p53c gene reassembly for wt and mutants, mutations are indicated in **red**. Each primer was prepared to give a 100 μM stock solution.

Amp^R, and *E. coli* T7 promoter genes**.** The ligated plasmid was transformed in *Escherichia*

A. p53c wt

SSSVPSQKTYQGSYGFRLGFLHSGTAKSVTCTYSPALNKMFCQLAKTCPVQLWVDSTPPP
GTRVRAMAIYKQSQHMTEVVRRCPHHERCSDSDGLAPPQHLIRVEGNLRVEYLDDRNTFR
HSVVVPYEPPEVGSDCTTIHYNYMCNSSCMGGMNRRPILTIITLEDSSGNLLGRNSFEVR
VCACPGRDRRTEEENL

B. p53c P223A ΔS7S8 (loop mutant)

SSSVPSQKTYQGSYGFRLGFLHSGTAKSVTCTYSPALNKMFCQLAKTCPVQLWVDSTPPP
GTRVRAMAIYKQSQHMTEVVRRCPHHERCSDSDGLAPPQHLIRVEGNLRVEYLDDRNTFR
HSVVVPYEP**A**CTTIHYNYMCNSSCMGGMNRRPILTIITLEDSSGNLLGRNSFEVR
VCACPGRDRRTEEENL

C. P53c Quad Mutant

SSSVPSQKTYQGSYGFRLGFLHSGTAKSVTCTYSPALNK**L**FCQLAKTCPVQLWVDSTPPPGT
RVRAMAIYKQSQHMTEVVRRCPHHERCSDSDGLAPPQHLIRVEGNLR**A**EYLDDRNTFRHS
VVVPYEPPEVGSDCTTIHYNYMC**Y**SSCMGGMNRRPILTIITLEDSSGNLLGR**D**SFEVRVC
ACPGRDRRTEEENL

Table 2. Amino acid sequence for p53c wild type (**A**.), quad mutant (**B.**), and loop mutant (**C.**). Mutations are indicated in **red**.

coli strain DH10B. Plasmid purification (QIAprep Spin Miniprep Kit, Qiagen) was followed by analytical digests with *Pci*I restriction enzyme (NEB). The recovered plasmid, pET11a-[p53C], was sequenced (Genewiz) using T7 promoter primer (5'-TAA TAC GAC TCA CTA TAG GG-3').

2.2 Protein Expression and Purification. Protein variants were expressed in *E. coli* strain BL21(DE3) and incubated at 37 ºC until induction with IPTG (0.10 mM) at OD_{600} 0.7 – 1.0, followed by overnight growth between 25-30 ºC. Cells were harvested by centrifugation and sonicated in lysis buffer (50 mM Tris•HCl, pH 8, 300 mM NaCl, 10 mM imidazole, 2 mM β-mercaptoethanol, and 0.10 mM ZnCl). The protein was purified using Ni^{2+} affinity. This was achieved upon addition of 50% slurry of Ni-NTA agarose (Qiagen) to supernatant after 4 ºC incubation for 1 h before loading on 10 mL fitted chromatography column (Bio-Rad). Wash buffer (50 mM Tris•HCl pH 8, 300 mM NaCl, 20 mM imidazole, 2 mM βME, 0.10 mM

ZnCl) was applied to the column, followed by elution buffer (50 mM Tris•HCl pH 8, 300 mM NaCl, 250 mM imidazole, 2 mM βME, 0.10 mM ZnCl). Protein concentration was determined both by spectrophotometric measures [ε_{280} (loop mutant) 17,210 M^{-1} cm^{-1}; ε_{280} (quad mutant) 18,490a M^{-1} cm^{-1}) obtained from Scripps Protein Calculator] and a Bradford Assay (Bio-Rad). TEV (Tobacco Etch Virus) protease cleavage reactions contained 5 mM DTT and varied protease aliquots in 3 h increments at temperatures ranging from 4-30 ºC. TEV reactions were exchanged into lysis buffer using PD-10 columns (GE Healthcare) followed by the aforementioned Ni^{2+} affinity chromatography, where the initial flow-through contains the His_6-cleaved target protein while TEV protease binds to the column due to an intrinsic His_6-tag.

2.3 Circular Dichroism . CD spectra were obtained with an AVIV 202 Circular Diochroism Spectrometer (AVIV Biomedical, Lakewood NJ) at the Analytical Spectroscopy Laboratory (The Ohio State University Chemistry Department). Wavelength scans were obtained from 200-400 nm, 5 s average readings, with a total of 3 scans. One mm QS cuvettes (Hellma Cells, Inc., Plainview, NY) were used for all studies. Thermal melts were carried out with a temperature range of 25-95 ºC (1º per s). Samples were exchanged in CD buffer (50 mM sodium phosphate, pH 7.2, 100 mM NaCl, 1 mM TCEP, and 1 mM ZnCl) using PD-10 chromatography columns (GE Healthcare) prior to CD studies.

CHAPTER 3. RESULTS AND DISCUSSION

3.1 p53c Gene Subcloning. The overall cloning scheme is depicted in **Figure 8**. Originally, an *Nde*I restriction site was found in the mid-section of the p53c gene that was incompatible with the intended cloning sites. This restriction site was later removed by incorporating a silent mutation from a re-ordered oligonucleotide. Gel electrophoresis of the PCR products from the gene reassemblies and amplifications are shown in **Figure 9**. The analytical digest to confirm authentic clones involves one restriction enzyme, *Pci*I, which provides for an efficient and easy digest set-up. Both the loop and quad mutant p53c genes have been subcloned into pET11a.

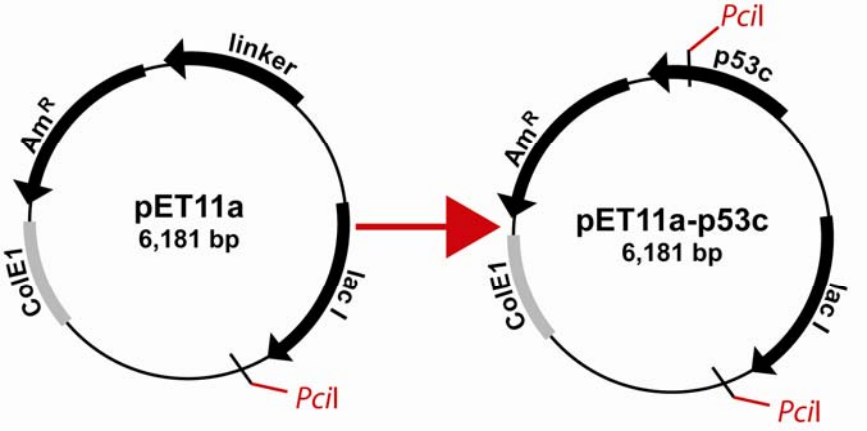

Figure 8. p53c cloning scheme. Each p53c gene variant (~650 bp) is inserted in to an overexpression vector, pET11a. Matching restriction sites (***Pci*I**) result when the cloning is a success.

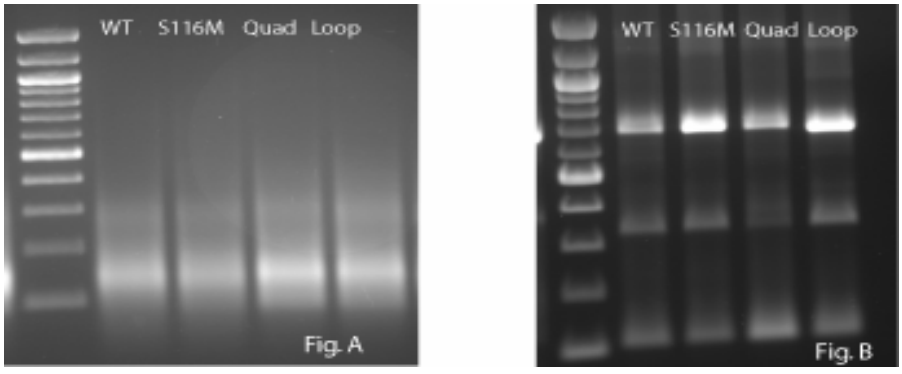

Figure 9. Gel Electrophoresis: 1% agarose analytical gel. A. PCR gene reassembly of p53c variants using Taq polymerase. **B**. PCR amplification of gene reassembly in **A**.

3.2 Protein Expression and Purification

3.2.1 Loop Mutant. The loop mutant (23.8 kDa) was the first variant expressed (**Fig. 10**) in *E. coli* BL21(DE3) for this study. Substantial aggregation was noticed throughout purification. In addition, impurities (~160 kDa) from *E. coli* that exhibit Ni^{2+} binding affinity have resulted in all purifications. Attempts to cleave the N-terminal fusion His_6-tag using TEV (Tobacco Etch Virus) protease has proved unsuccessful for the loop mutant. Varied temperatures, protease concentrations, and reactions times were applied. AcTEV (Invitrogen) was also used, but did not produce cleavage as well. As a potential solution, a TEV linker region, GSSG, was introduced between the N-terminal p53c residue and the TEV recognition site to potentially extend the TEV recognition site for access by the protease. The linker did not promote cleavage. As final alternative, TAGzyme (Qiagen) will be used to remove the His_6-tag. TAGZyme (**Fig. 10**) is a cleavage kit often used for cleaving His_6-tags from proteins intended for structural studies when other cleavage options are not possible. Perhaps, the TEV protease recognition site is folding in with the protein, making TEV cleavage inaccessible.

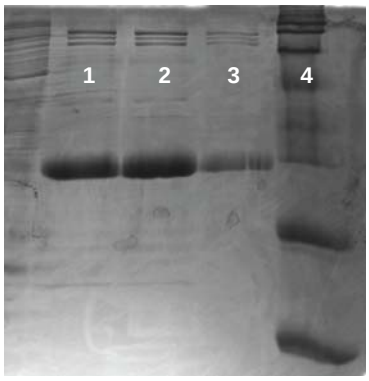

Figure 9. 18% SDS-PAGE. Lanes 1-3 depict sequential elutions from Ni^{2+} binding affinity column of p53c Loop mutant (23.8 kDa). The purification results were referenced with MW-marker, RPN-800. (lane 4).

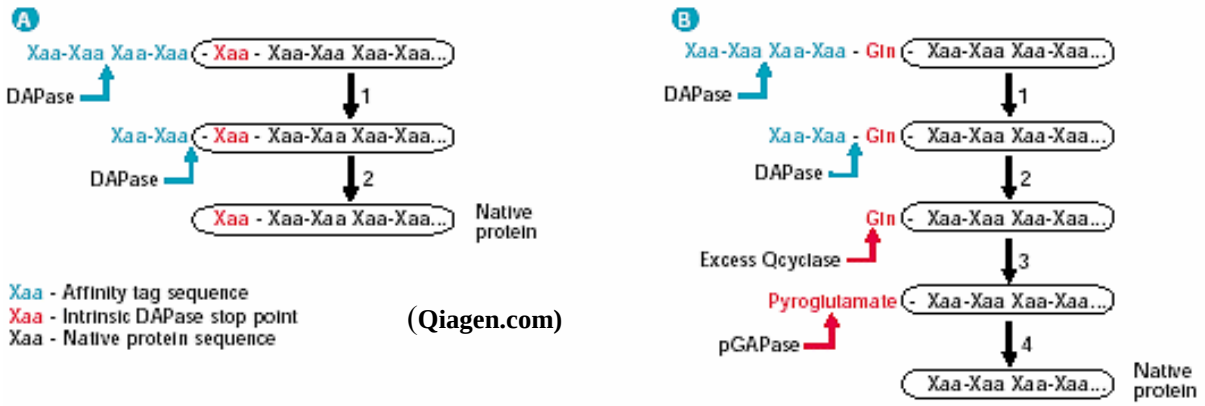

Figure 10. TAGZyme cleavage scheme. DAPase enzyme cleaves dipeptides from N-terminals of proteins until a natural stop point is reached, as seen in **A,** to produce the native protein. **B**. For proteins that do not contain a DAPase natural stop point, a Gln residue is introduced at an odd position directly before the native protein sequence and after the His6-tag. Excess Qcyclase then converts the Gln to pyroglutamine, which halts DAPase cleavage. pGAPase removes the converted stop point, resulting in the native protein.

3.2.2 Quad Mutant. The quad mutant was the second p53c variant expressed in this study (**Fig. 11**). Aggregation was not observed throughout purification. Surprisingly, TEV protease was able to cleave the His_6-tag from the N-terminus. However, expression levels are relatively low compared to the loop mutant.

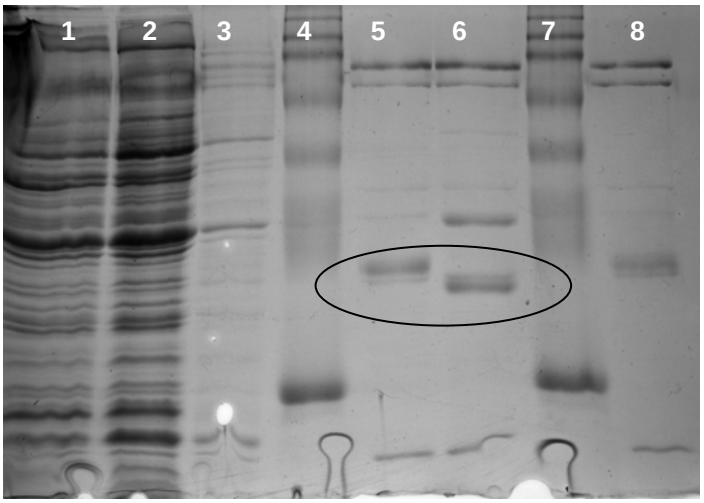

Figure 11. 18% SDS-PAGE of p53c quad expression and purification. Lane 5 is the uncut quad (24.3 kDa) and Lane 6 represents the cleaved quad mutant (22.4 kDa) using TEV protease. Lanes 4 and 7 contain MW marker, RPN 800. Lanes 1-3 represent supernatant, flow-through from Ni-NTA column, and wash from column, respectively.

3.3 Circular Dichroism Spectroscopy. Circular Dichroism (CD) Spectroscopy is a useful tool for determining the secondary structure of a protein and performing thermal denaturation studies. CD uses circularly polarized light to produce a signal with varied magnitudes based on biomolecular structures (e.g. β-sheets, α-helices, or random coil) that have a signature response. The signal indicates an average of the entire molecular population, where the peptide bond acts as the chromophore. CD spectrum was obtained for the quad and loop variants at varied concentrations (15.1 and 27.2 μM for loop; 22.6 and 26.5 μM for quad). The lower concentrations from each variant represent a separate stock solution from prior expression attempts shown to contain minimal impurities. A Bradford Assay was used to determine the initial concentrations of these protein solutions before concentrating down in a

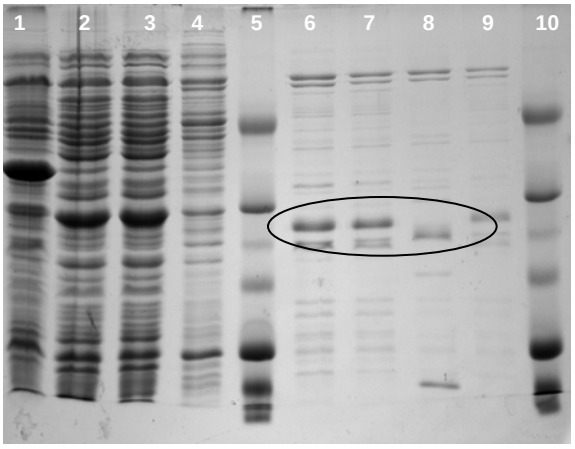

Figure 12. 12.5% SDS-PAGE of p53c quad (24.3 kDa) and loop (23.8 kDa) expression and purification. Lanes 6 and 7 represent loop mutant in elution and CD buffer, respectively. Lane 8 contains quad mutant in CD buffer. Lanes 5 and 10 contain MW marker, RPN 755. Overall impurities for each mutant is substantial, coupled with poor expression levels. Lanes 1-4 represent pellet from centrifugation, supernatant, flow-through from Ni-NTA column, and wash, respectively, from loop purification.

YM-10 spin column. The higher concentrations of each variant were determined by UV-Vis spectrophotometry in a 50 µL quartz cuvette. Upon observing the SDS-PAGE analysis (**Fig. 12**), significant impurities exist in both p53c mutant solutions. Therefore, the CD spectrum (**Fig. 13**) cannot be relied upon, as the impurities may have secondary structure causing a distortion in CD signal from the target protein. The loop mutant has significant impurities (~30 kDa). Initial thermal melts were inconclusive since the data collection was too fast (1 ºC per s) for meaningful data.

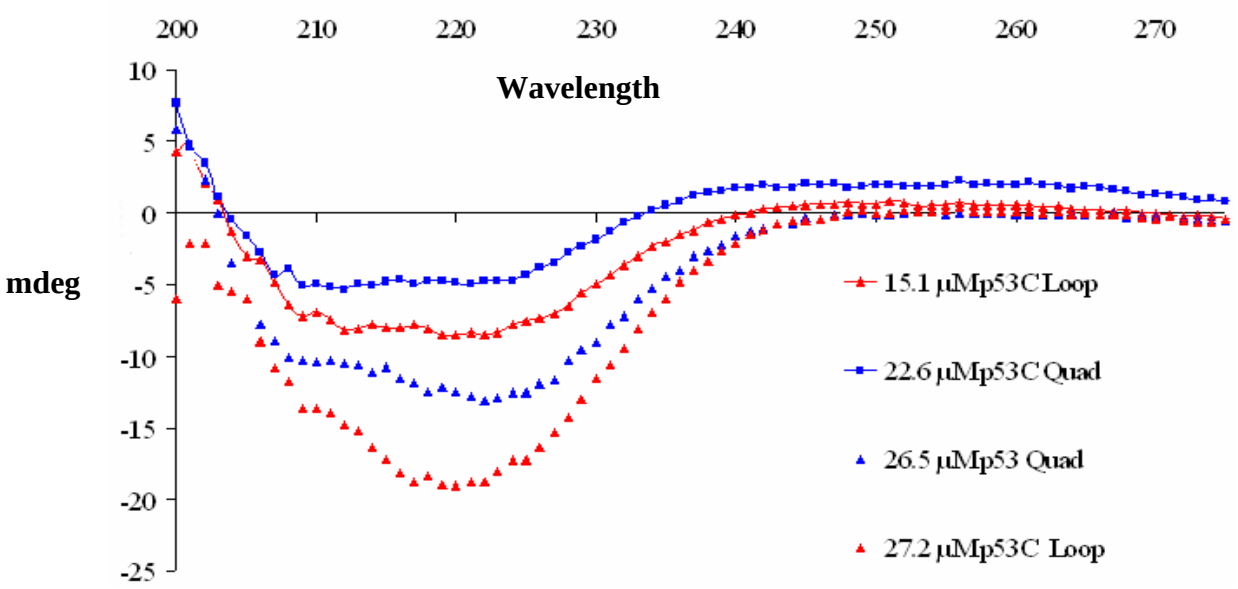

Figure 13. CD spectrum (mdeg vs. wavelength) of p53c loop and quad mutants. Mild signals were produced for the wavelength scan of each variant. Although loop seems to produces the strongest signal, it also the least pure. Thus, this data is inconclusive for confirming the secondary structural attributes of each variant.

3.4 Discussion. The core domain of p53 has significant influence on the thermodynamics of full-length p53. As result, mutations within this domain largely dictate either the foldedness or DNA-binding of this transcription factor that is centrally-positioned in a complex

signaling pathway responsible for cell-cycle control and ultimately, over 50% of tumor-derived human cancers. This study seeks to compare a previously engineered "super-stable" mutant, or quad mutant, with a loop mutant that is computationally predicted to surpass the quad mutant in stability. The implications of this study may provide functional and structural insight between the effects of mutating a peripheral structural motif (loop mutant) and the β-sheet scaffold (quad) of a fairly simple protein domain. In a broader sense, if the loop mutant is not only thermodynamically more stable than the previously tested quad mutant, but functionally active, the loop mutation may be an amenable alternative for full-length p53 studies, which are normally limited due the wild-type marginal stability. In addition, proving an increased stability of the loop mutant compared to quad, as previously predicted by MD simulations, may instill a certain confidence in using MD simulations as an indicator for actual relative stability. Of course, more studies of this sort that tests for actual relative stabilities between proteins, or any other macromolecule, would provide an elevated confidence in using MD simulations in a high-throughput format.

This study has successfully expressed each p53c variant, albeit purification and expression optimization is still underway to provide adequate amounts of each protein solution at high purity. In addition, a cleaved version (no His_6-tag) of the loop is desired in order for accurate comparisons with prior studies that do not have this affinity tag on p53c variants. The anomalous TEV cleavage, or lack thereof, between the two p53c variants of this study is interesting. It is possible that the His_6-tag is being folded with the loop protein, thereby blocking the TEV recognition site for cleavage. Considering this, significant structural differences between the two mutants seem apparent before any biophysical characterization. Thus, running the various stability tests while identifying structural

attributes of these variants will entail both the cleaved and un-cleaved versions. Eventually, we hope to develop novel insight for additional forces that stabilize p53.

3.5 Future Direction. Expression and purification of p53c quad and loop mutants are currently being optimized. Cleavage of the His_6-tag will be attempted with TAGZyme (**3.2.1**) for the loop mutant in order to achieve native structure prior to biophysical studies. When sufficient amounts of each variant are attained with adequate purity, thermal studies involving urea- and thermal-induced denaturation experiments will be run using CD spectroscopy and fluorimetry. A Hydrogen/Deuterium exchange experiment using NMR is planned for each variant in order to measure backbone protection of amide protons resulting from a folded state or at least, secondary structure. It is also our interest to obtain the crystal structure of the loop mutant, since this variant has not been characterized. An *in vivo* screen is currently being optimized by a graduate student, Brinda Ramasubramanian, in our group to test the functionality of the p53c mutants.

References

1. Kraulis, P. J., Molscript - a Program to Produce Both Detailed and Schematic Plots of Protein Structures. *Journal of Applied Crystallography* **1991,** 24, 946-950.
2. Marine, J. C.; Francoz, S.; Maetens, M.; Wahl, G.; Toledo, F.; Lozano, G., Keeping p53 in check: essential and synergistic functions of Mdm2 and Mdm4. *Cell Death and Differentiation* **2006,** 13, (6), 927-934.
3. Ang, H. C.; Joerger, A. C.; Mayer, S.; Fersht, A. R., Effects of Common Cancer Mutations on Stability and DNA Binding of Full-length p53 Compared with Isolated Core Domains. *Journal of Biological Chemistry* **2006,** 281, (31), 21934-21941.
4. Wang, P.; Reed, M.; Wang, Y.; Mayr, G.; Stenger, J. E.; Anderson, M. E.; Schwedes, J. F.; Tegtmeyer, P., p53 domains: structure, oligomerization, and transformation. *Molecular and cellular biology* **1994,** 14, (8), 5182-91.
5. Bullock, A. N.; Henckel, J.; DeDecker, B. S.; Johnson, C. M.; Nikolova, P. V.; Proctor, M. R.; Lane, D. P.; Fersht, A. R., Thermodynamic stability of wild-type and mutant p53 core domain. *Proceedings of the National Academy of Sciences of the United States of America* **1997,** 94, (26), 14338-14342.
6. Vogelstein, B.; Lane, D.; Levine, A. J., Surfing the p53 network. *Nature* **2000,** 408, (6810), 307-10.
7. Cho, Y.; Gorina, S.; Jeffrey, P. D.; Pavletich, N. P., Crystal structure of p53 tumor suppressor-DNA complex: understanding tumorigenic mutations. *Science (Washington, DC, United States)* **1994,** 265, (5170), 346-55.
8. Friedler, A.; Veprintsev, D. B.; Hansson, L. O.; Fersht, A. R., Kinetic instability of p53 core domain mutants - Implications for rescue by small molecules. *Journal of Biological Chemistry* **2003,** 278, (26), 24108-24112.
9. Bell, S.; Klein, C.; Muller, L.; Hansen, S.; Buchner, J., p53 contains large unstructured regions in its native state. *Journal of Molecular Biology* **2002,** 322, (5), 917-927.
10. Hainaut, P.; Hollstein, M., p53 and human cancer: the first ten thousand mutations. *Advances in cancer research* **2000,** 77, 81-137.
11. Olivier, M.; Eeles, R.; Hollstein, M.; Khan, M. A.; Harris, C. C.; Hainaut, P., The IARC TP53 database: New Online mutation analysis and recommendations to users. *Human Mutation* **2002,** 19, (6), 607-614.

12. Joerger, A. C.; Ang, H. C.; Fersht, A. R., Structural basis for understanding oncogenic p53 mutations and designing rescue drugs. *Proceedings of the National Academy of Sciences of the United States of America* **2006,** 103, (41), 15056-15061.

13. Joerger, A. C.; Ang, H. C.; Veprintsev, D. B.; Blair, C. M.; Fersht, A. R., Structures of p53 cancer mutants and mechanism of rescue by second-site suppressor mutations. *Journal of Biological Chemistry* **2005,** 280, (16), 16030-16037.

14. Kitayner, M.; Rozenberg, H.; Kessler, N.; Rabinovich, D.; Shaulov, L.; Haran, T. E.; Shakked, Z., Structural basis of DNA recognition by p53 tetrarners. *Molecular Cell* **2006,** 22, (6), 741-753.

15. Bullock, A. N.; Henckel, J.; Fersht, A. R., Quantitative analysis of residual folding and DNA binding in mutant p53 core domain: definition of mutant states for rescue in cancer therapy. *Oncogene* **2000,** 19, (10), 1245-1256.

16. Nikolova, P. V.; Henckel, J.; Lane, D. P.; Fersht, A. R., Semirational design of active tumor suppressor p53 DNA binding domain with enhanced stability. *Proceedings of the National Academy of Sciences of the United States of America* **1998,** 95, (25), 14675-14680.

17. Brachmann, R. K.; Yu, K. X.; Eby, Y.; Pavletich, N. P.; Boeke, J. D., Genetic selection of intragenic suppressor mutations that reverse the effect of common p53 cancer mutations. *Embo Journal* **1998,** 17, (7), 1847-1859.

18. Eldeiry, W. S.; Kern, S. E.; Pietenpol, J. A.; Kinzler, K. W.; Vogelstein, B., Definition of a Consensus Binding-Site for P53. *Nature Genetics* **1992,** 1, (1), 45-49.

19. Dehner, A.; Klein, C.; Hansen, S.; Muller, L.; Buchner, J.; Schwaiger, M.; Kessler, H., Cooperative binding of p53 to DNA: Regulation by protein-protein interactions through a double salt bridge. *Angewandte Chemie-International Edition* **2005,** 44, (33), 5247-5251.

20. Brooks, B. R.; Bruccoleri, R. E.; Olafson, B. D.; States, D. J.; Swaminathan, S.; Karplus, M., Charmm - a Program for Macromolecular Energy, Minimization, and Dynamics Calculations. *Journal of Computational Chemistry* **1983,** 4, (2), 187-217.

21. Pan, Y.; Ma, B.; Levine Arnold, J.; Nussinov, R., Comparison of the human and worm p53 structures suggests a way for enhancing stability. *Biochemistry* **2006,** 45, (12), 3925-33.

22. Schumacher, B.; Hofmann, K.; Boulton, S.; Gartner, A., The C. elegans homolog of the p53 tumor suppressor is required for DNA damage-induced apoptosis. *Current Biology* **2001,** 11, (21), 1722-1727.

23. Huyen, Y.; Jeffrey, P. D.; Derry, W. B.; Rothman, J. H.; Pavletich, N. P.; Stavridi, E. S.; Halazonetis, T. D., Structural Differences in the DNA Binding Domains of Human p53 and Its C. elegans Ortholog Cep-1. *Structure (Cambridge, MA, United States)* **2004,** 12, (7), 1237-1243.